Article

Enantio- and Regioselective Ir-catalyzed Hydrogenation of Di- and Trisubstituted Cyclohexenes

Byron K. Peters, Jianguo Liu, Cristiana Margarita, Wangchuk Rabten, Sutthichat Kerdphon, Alexander Orebom, Thomas Morsch, and Pher G. Andersson

J. Am. Chem. Soc., **Just Accepted Manuscript** • DOI: 10.1021/jacs.6b07291 • Publication Date (Web): 22 Aug 2016

Enantio- and Regioselective Ir-catalyzed Hydrogenation of Di- and Trisubstituted Cyclohexenes

Byron K. Peters,[a, ‡] Jianguo Liu,[a, ‡] Cristiana Margarita,[a, ‡] Wangchuk Rabten,[a, ‡] Sutthichat Kerdphon,[a, ‡] Alexander Orebom,[a] Thomas Morsch,[a] and Pher G. Andersson*[,a].

[a]Department of Organic Chemistry, Stockholm University, Arrhenius-laboratory, 10691 Stockholm, Sweden.

[‡]These authors contributed equally.

ABSTRACT: A number of cyclic olefins were prepared and evaluated for the asymmetric hydrogenation reaction using novel N,P-ligated iridium imidazole based catalysts (Crabtree type). The diversity of these cyclic olefins spanned those having little functionality to others bearing strongly coordinating substituents and heterocycles. Excellent enantioselectivities were observed both for substrates having little functionality (up to >99 % ee) as well as substrates possessing functional groups several carbons away from the olefin. Substrates having functionalities such as carboxyl groups, alcohols or heterocycles in the vicinity of the C=C bond, where hydrogenated in high enantiomeric excess (up to >99 % ee). The hydrogenation was also found to be regio-selective and by control of the reaction conditions, selective hydrogenation of one of two tri-substituted olefins can be achieved. Furthermore, tri-substituted olefins can be selectively hydrogenated in the presence of tetra-substituted olefins.

Introduction

The substituted cyclohexane unit is an important scaffold in natural products and total synthesis.[1] The majority of these motifs have stereogenic centers on the cyclohexane, for example: sesquiterpenes Eudesmane, Ere-mophilan, and Frovatriptan, a drug for the treatment of migraines (Figure 1).[2]

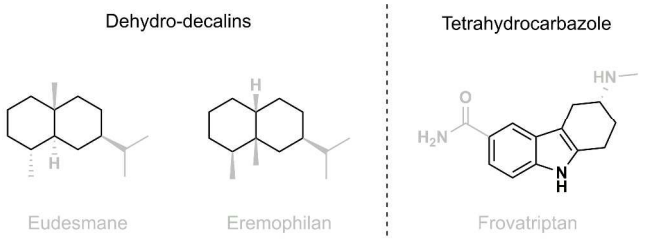

Figure 1: Chiral cyclohexanes in nature

A number of stereoselective methods have been developed to prepare chiral carbocycles including cyclohexanes. The most successful are using a chiral catalyst, such as: Diels-Alder[3], polyene cyclization, Robinson annulation, and organocatalyzed domino or cascade reactions[1, 4]. While these reactions are important and have been used to prepare a number of natural products and pharmaceuticals[5], their generality in terms of their substrate scope is not optimal. For example, a high degree of functionality in the starting materials is required (domino and to a lesser extent the Diels-Alder), some are only amenable to the preparation of two or more fused rings (polyene and Robinson annulation), not to mention the high catalyst loading that accompanies a majority of the organocatalytic methods (> 5 mol%).

In short, there lacks a general method to prepare these important structures having either minimal functionality or those which are functionalized and even bearing heterocyclic units. The iridium catalyzed asymmetric hydrogenation is a mild and efficient method to hydrogenate olefins for the preparation of chiral molecules, typically in high enantiomeric excess. More importantly, using N,P-ligands, minimally functionalized chiral molecules can be prepared in high optical purity and yield. In more recent studies these Ir-N,P catalysts have been successfully used for hydrogenation of substrates having a wide range of functional groups at the olefin. Therefore, one could envisage using the Ir-N,P strategy in the hydrogenation of easily prepared cyclohexene precursors.

The asymmetric hydrogenation as a means of installing stereogenic centers in cyclic systems has been investigated to some extent.[6] In particular, heterocycles have been hydrogenated with high levels of enantioselectivity.[7] On the other hand, there are surprisingly few examples for the hydrogenation of unsaturated carbocycles. The asymmetric hydrogenations of 2,3-benzofused derivatives (Figure 2) having 1[8] and 6[8f, 9] substitution, resulted in moderate to good enantioselectivity.

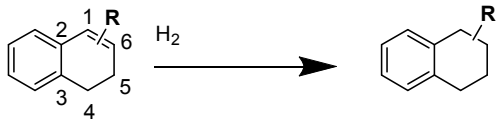

Figure 2: Chiral cyclohexanes by hydrogenation

Successful examples for the asymmetric hydrogenation of compounds possessing more than one prochiral olefin are very rare[8d] and have been mainly focused on conjugated 1,3-dienes[10], hence convergent approaches are sometimes employed in total synthesis.[11] Therefore, 1,4-cyclohexadiene substrates afford an interesting opportunity for the preparation of multiple stereogenic centers.

In this work, we have developed a facile and enantioselective method to prepare a diversity of chiral cyclic molecules from their corresponding cyclohexenes (Class 1-3, Figure 3).

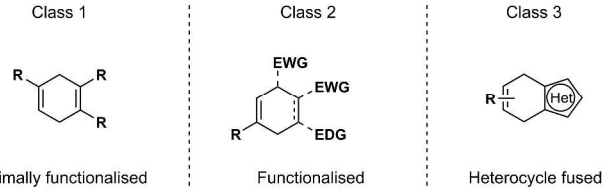

Figure 3: Substrate classes

Discussion

Ligand design has always been a challenge for asymmetric catalysis. It is often necessary that the electronic and steric properties of the substituents on the ligand can be varied in order to gain optimal enantioselectivity.[12] We have shown previously that substrates of class 1 are hydrogenated in high yield and enantiomeric excess with catalysts **i** and **ii**, bearing a thiazole and imidazole ligand, respectively (Figure 4).[13] Moreover, acid labile substrates such as enol ethers were tolerated by catalyst **ii**. A surprising outcome since related N,P-ligated iridium catalysts have been shown to produce Ir-polyhydride species in solution when treated with hydrogen[14], which more recently have been revealed to be appreciably acidic.[15] This prompted us to investigate the influence of the substituent on the imidazole in the asymmetric hydrogenation reaction. The imidazole ligand is biaryl in nature, and biaryls possess an interesting chemistry, particularly with respect to substituent effects.[16] In this study we present the hydrogenation of a broad range of cyclohexene substrates having various degrees of functionalization (Figure 3) with novel imidazole-based N,P-iridium catalysts (Figure 4).

Some model substrates were chosen to evaluate the imidazole catalysts (Table 1). Monocyclic dihydrobenzene **1a** and tetrahydronaphthalenes **2a** and **3a** are hydrogenated in essentially full conversion using 0.5 mol % catalyst loading. While the reactivity of the catalysts was independent of the substituent on the imidazole, the enantioselectivity showed a strong dependence. Having a 4-methyl substitution (cat-**iii**) is beneficial, compared to 4-H (cat-**ii**). Somewhat higher enantioselectivity is observed in most cases. The 2-methyl substituent (cat-**iv**), has higher enantioselectivity for the naphthalene type substrates than catalysts **ii** and **iii**, however, significantly lower selectivity was observed for the dihydrobenzene type substrate (compare entries 2 and 3, cat-**ii** and cat-**iii** with entry 1, cat-**iv**). Having both 2- and 4-methyl substitution (cat-**v**) offered high selectivity. Comparably high and in some cases significantly higher selectivity was observed compared to catalysts **ii**-**iv**. Interestingly, having a 4-methoxy substituent (cat-**vi**) did not result in the same benefits as the 4-methyl (cat-**iii**) and lower selectivity is obtained compared to cat-**ii**. The 2- and 4-dimethoxy version (cat-**vii**), however, furnished the hydrogenated products in excellent enantioselectivity, similarly to the 2,4-dimethyl counterpart, cat-**v**.

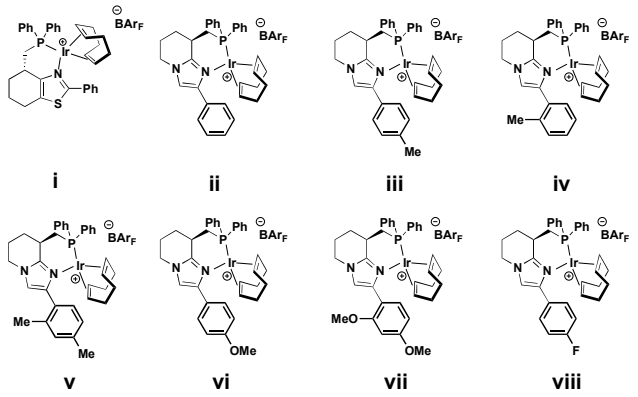

Figure 4: Catalysts used in this study

Other substrates, having a minimal functionalization were screened (Table 2). High enantioselectivities were obtained regardless of the substituent on the substrate (Me, *i*-Bu, OMe, *n*-Pent, *i*-Pr, Bn). The 2,4-dimethyl imidazole catalyst **v** performed well, being the most selective catalysts for a majority of the substrates (entries 1-11, 13-16, 18-20 and 22-23). In only a few instances did other catalysts such as the thiazole cat-**i** (entries 12, 17 and 21), and the 2,4-dimethoxy cat-**vii** (entries 24-25), produce higher enantioselectivities than cat-**v**. In each case, the hydrogenations with cat-**v** proceeded smoothly, tolerating even acid labile substrates (entries 8-14 and 17-22), problematic substrates for many iridium N,P catalysts. Furthermore, the thermodynamically less stable *trans* isomers are predominantly formed for 1,3-substitutions. This is in line with catalyst control over substrate control, typically observed for N,P-ligated Ir-catalysts.[17]

Table 1: Evaluation of catalysts in the asymmetric hydrogenation of unsaturated carbocycles[a,b,c]

Entry	Substrate	Product	i		ii		iii		iv		v		vi		vii		viii	
			conv.	ee (%)	conv.	ee (%)	conv.	ee (%)	conv.	ee (%)	conv.	ee (%)	conv.	ee (%)	conv.	ee (%)	conv.	ee (%)
1	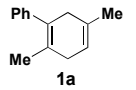 **1a**	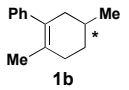 **1b**	99	92	99	79	99	81	99	67	**99**	**93**	99	65	**59[d]**	**94**	99	35
2	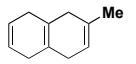 **2a**	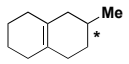 **2b**	99	87	99	65	99	62	99	81	**99**	**86**	99	43	**99**	**94**	99	17
3	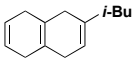 **3a**	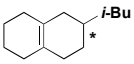 **3b**	99	92	99	65	99	78	99	88	**99**	**84**	99	59	**99**	**92**	99	26

[a]Reaction conditions: 0.125 mmol of substrate, 0.5 mol % catalyst, 1 mL of CH_2Cl_2, 50 bar of H_2, 17 h, rt, unless stated otherwise in the supplementary information. [b]All examples are hydrogenated to full conversion where enantioselectivity is reported, which was determined by ^{1}H NMR spectroscopy. No side products were detected. [c]Determined by HPLC or GC analyses using a chiral stationary phase. [d]Only starting material was detected other than the product.

Table 2: Asymmetric hydrogenation of minimally functionalized carbocycles (Class 1)[a]

Entry	Substrate	Product[b]	Catalyst	Yield (%)[c]	ee (%)[d]
1	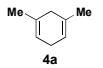 4a	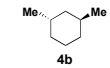 4b	**v**	99[e]	99
2	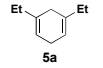 5a	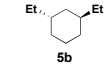 5b	**v**	99[e,f]	94
3	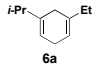 6a	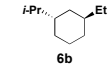 6b	**v**	99[e,f]	96
4	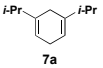 7a	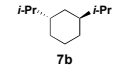 7b	**v**	76[f]	99
5	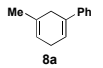 8a	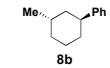 8b	**v**	91	99
6	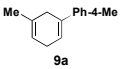 9a	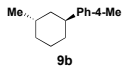 9b	**v**	81	99
7	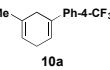 10a	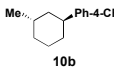 10b	**v**	99[e]	99
8	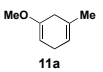 11a	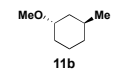 11b	**v**	99[e]	99
9	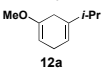 12a	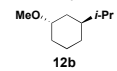 12b	**v**	99[e,f]	99
10	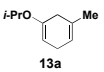 13a	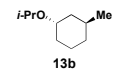 13b	**v**	71[f]	98
11	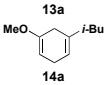 14a	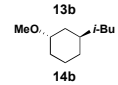 14b	**v**	68	99
12	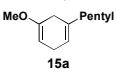 15a	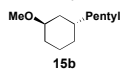 15b	**i**	81	98
13	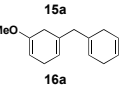 16a	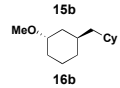 16b	**v**	95	99
14	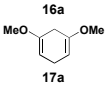 17a	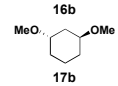 17b	**v**	99[e]	99
15	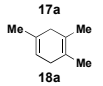 18a	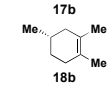 18b	**v**	99[e]	94
16	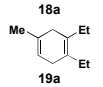 19a	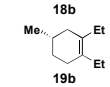 19b	**v**	99[e]	99
17	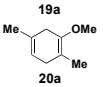 20a	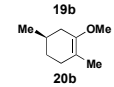 20b	**i**	99[e]	98
18	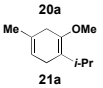 21a	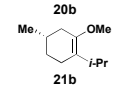 21b	**v**	99[e]	92
19	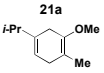 22a	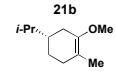 22b	**v**	99[e]	98
20	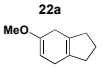 23a	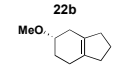 23b	**v**	82	98
21	24a	24b	**i**	98	99
22	25a	25b	**v**	72	99
23	1a	1b	**v**	97	93
24	2a	2b	**vii**	98	94
25	3a	3b	**vii**	98	92

[a]Reaction conditions: 0.125 mmol of substrate, 0.5 mol % catalyst, 1 mL of CH_2Cl_2, 50 bar of H_2, 17 h, rt, unless stated otherwise in the supporting information. [b]Predicted absolute stereochemistry for the major product (>90% *trans* observed where applicable, unless otherwise stated). [c]Isolated yield unless otherwise specified. [d]Determined by HPLC or GC analyses using a chiral stationary phase. [e]Conversion determined by ^{1}H NMR spectroscopy. [f]Selectivity to trans <80 %.

Substrates with side chains bearing functional groups such as OH, OTBDMS and COOMe (Table 3) were also tolerated and furnished the saturated products in high enantiomeric excess (*trans* isomer). Catalyst **v** provided the best selectivity in most cases, with ee's exceeding 90 %.

Table 3: Asymmetric hydrogenation of unsaturated carbocycles having non-ring bound functional groups (Class 1 extended)[a]

Entry	Substrate	Product[b]	Catalyst	Yield (%)[c]	ee (%)[d]
1	26a	26b	**v**	84	99
2	27a	27b	**v**	86[e]	99
3	28a	28b	**v**	87[e]	99
4	29a	29b	**ix**[f]	97[e]	92
5	30a	30b	**v**	79[e]	97

[a]Reaction conditions: 0.125 mmol of substrate, 0.5 mol % catalyst, 1 mL of CH_2Cl_2, 50 bar of H_2, 17 h, rt, unless stated otherwise in the supporting information. [b]Predicted absolute stereochemistry for the major product (>90% *trans* observed where applicable, unless otherwise stated). [c]Isolated yield. [d]Determined by HPLC or GC analyses using a chiral stationary phase. [e]Selectivity to *trans* <80 %. [f]See supporting information.

Substrates having functional groups directly attached to the carbocycle were also screened. Interestingly, despite the steric encumbrance that the carboxyl groups impose, fantastic enantioselectivity could be maintained using cat-**v**.

Table 4: Asymmetric hydrogenation of unsaturated carbocycles having ring bound functional groups (Class 2)[a]

Entry	Substrate	Product[b]	Catalyst	Yield (%)[c]	ee (%)[d]
1	31a	31b	**i**	91[e]	99
2	32a	32b	**x**[f]	98[e]	99
3	rac-33a	33b + 33c	**v**	98[g]	99
4	34a	34b	**v**	99[h]	97

[a]Reaction conditions: 0.125 mmol of substrate, 0.5 mol % catalyst, 1 mL of CH_2Cl_2, 50 bar of H_2, 17 h, rt, unless stated otherwise in the supporting information. [b]Predicted absolute stereochemistry for the major product (>90% *trans* observed where applicable, unless otherwise stated). [c]Isolated yield unless otherwise specified. [d]Determined by HPLC or GC analyses using a chiral stationary phase. [e]>95% *trans*-dimethyl product. [f]See supporing information. [g]For both *cis*-fused diastereomers (1:1). [h]Conversion determined by ^{1}H NMR spectroscopy.

A number of heterocyclic substrates were also evaluated (Table 5). These substrates were found to require higher catalyst loading (1-2 mol %), nevertheless high ee's were obtained (up to 99 %) for both 5- and 6- substitutions (indole nomenclature). Catalyst **v** had good selectivity for the Me and OMe substituted indoles and carbazoles (entries 1, 4, 5 and 7). However, the longer carbon chains (*n*-Bu, *n*-Hex) on the indole type substrates were handled better with the thiazole catalyst **i** (entries 2 and 3), except in the case of the carbazole, where catalyst **ii** performed more satisfactorily (entry 6). Having a thiophene unit as a substituent was well tolerated by catalyst **i** (entry 8). No reduction of the pyrrole (entries 1-6), indole (entry 7) or thiophene (entry 8) was observed in any case.

Table 5: Asymmetric hydrogenation of unsaturated carbocycles having fused heterocycles (Class 3)[a]

Entry	Substrate	Product[b]	Catalyst	Yield (%)[c]	ee (%)[d]
1	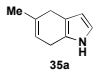 35a	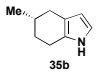 35b	**v**	98	99
2	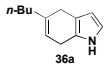 36a	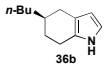 36b	**i**	85	90
3	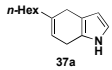 37a	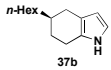 37b	**i**	83	92
4	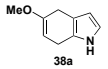 38a	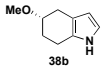 38b	**v**	99[e]	99
5	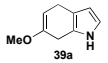 39a	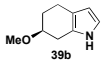 39b	**v**	99[e]	99
6	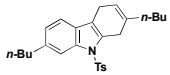 40a	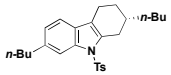 40b	**ii**	98	90
7	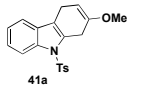 41a	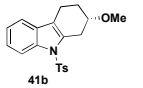 41b	**v**	99[e]	99
8	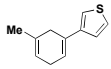 42a	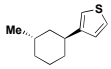 42b	**i**	99[e]	99

[a]Reaction conditions: 0.125 mmol of substrate, 0.5 mol % catalyst, 1 mL of CH_2Cl_2, 50 bar of H_2, 17 h, rt, unless stated otherwise in the supporting information. [b]Predicted absolute stereochemistry for the major product (>90% *trans* observed where applicable, unless otherwise stated). [c]Isolated yield unless otherwise specified. [d]Determined by HPLC or GC analyses using a chiral stationary phase. [e]Conversion determined by ^{1}H NMR spectroscopy.

Regioselectivity

Hydrogenations were observed to be regioselective, affecting only the di- and trisubstituted olefins at 50 bar of H_2. In addition to these findings, it was observed that control of the conditions using these new imidazole catalysts allowed for regioselectivity in the hydrogenation of two different trisubstituted olefins. This is in contrast to the relatively non-bulky Crabtree catalyst, which readily hydrogenates even more hindered olefins such as tetra-substituted C=C groups.[18] Compound **10a** (Table 6), bearing two trisubstituted olefins, was hydrogenated in full conversion to the corresponding saturated alkane **10b** with 50 bar H_2 over 17 hours. If the reaction time is lowered to 30 min, the reaction is nearly complete, however, a small amount the styrene like intermediate **10c** is observed. If the pressure is reduced to 5 bar of H_2 and the reaction allowed to proceed for 5 hours, substantially more of the styrene intermediate **10c** is observed.

The hydrogenation of compound **42a** was also observed to be amenable to regioselectivity reduction by varying the conditions of the reaction. At 50 bar of H_2, hydrogenation of both olefins takes place in 17 hours. However, by lowering the reaction time, the intermediate **42c** bearing the vinyl thiophene unit is obtained exclusively with good selectivity.

Table 6: Regioselective hydrogenations[a]

		pH_2/ bar	time/ min	 10c 42c	 10b 42b
1	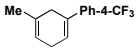 10a	5	30	94 (99% ee)	6
2	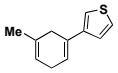 42a	50	300	83 (99% ee)	17

[a]Reaction conditions: 0.125 mmol of substrate, 0.5 mol % catalyst **v**, 1 mL of CH_2Cl_2, Conversion determined by ^{1}H NMR spectroscopy. Enantioselectivity determined by HPLC or GC analyses using a chiral stationary phase.

Aside from the obvious synthetic advantages to this regioselectivity, the relatively simple means to bring it about further caters to the utility of the methodology.

Mechanism and stereoselectivity

The mechanism of the asymmetric hydrogenation of trisubstituted olefins mediated by iridium N,P and C,N cationic catalysts has been extensively studied by means of DFT calculations and a catalytic cycle involving Ir^{III}/Ir^{V} has been proposed.[19] The likelihood of this reaction pathway has been supported both by more recent computational investigations[20] and experimental NMR studies by Pfaltz[21], reporting the identification of a fundamental intermediate, an Ir^{III} dihydride alkene complex. This species was shown to represent a resting state of the catalyst, requiring the coordination of an additional dihydrogen molecule, prior to the enantioselective migratory insertion step, generating intermediate **A** (Figure 5a).

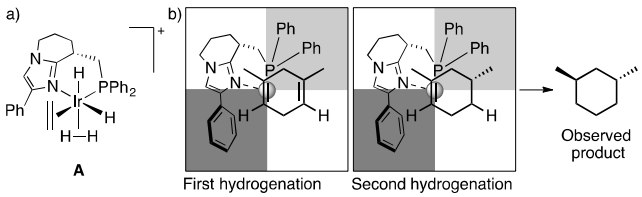

Figure 5. Selectivity model

The understanding of the reaction mechanism and the observation of the structure of intermediate **A** enabled the devel-

opment of a selectivity model, aimed to rationalize the stereochemical outcome of the asymmetric hydrogenation.[22] This quadrant model has proven able to predict the absolute configuration of the major enantiomer for a wide variety of saturated products. It is also suitable to explain the *trans* preference observed in the hydrogenation of cyclohexadienes.[13] The results suggest that the first hydrogenation product is dissociated and then coordinated again from the favored face of the second double bond, hence generating preferentially the *trans* isomer of the corresponding cyclohexane (Figure 5b).

The absolute configuration of three different cyclohexanes (Table 7) was assigned comparing their values of optical rotation to those available in the literature.[23] For all of the three cases, it was found that the major produced enantiomer matches the configuration estimated according to the selectivity model.

Table 7. Assigned absolute configurations[a]

		Absolute configuration	
		predicted from mechanistic model	observed
1	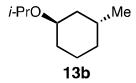 **13b**	(R)	(R)-(-)[22a]
2	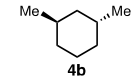 **4b**	(R)	(R)-(+)[22b]
3	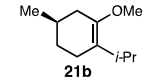 **21b**	(R)	(R)-(+)[b,22c]

[a]After hydrogenation employing catalyst *(S)*-**v** (Entry 1 and 2) or catalyst **i** (Entry 3). [b]See supporting information for experimental details.

Conclusion

A number of cyclic prochiral olefins were hydrogenated successfully (>99 conv., up to >99 % ee) using novel N,P-ligated iridium catalysts. The effect of the substituent on the aryl ring, flanking the imidazole ring had significant influence on the enantioselectivity of the catalyst. It was observed that having a 2,4-dimethyl aryl substitution furnished the best catalyst, tolerating a broad scope of cyclic substrates, furnishing the products with high enantioselectivity. Minimally functionalized substrates (Class 1) and those having functional groups not directly attached to the cycle were hydrogenated rapidly and in high ee. Substrates having functional groups and heterocycles attached to the unsaturated cycle, were hydrogenated slower, however, high enantioselectivity was maintained. It was also possible to attain remarkable regioselectivity between two trisubstituted olefins on cyclic diene structures, a goal met only by few catalysts so far. Mechanistic insight aided to rationalize the stereochemical outcome of the reaction and observed absolute configurations were found in agreement to the selectivity model.

ASSOCIATED CONTENT

Supporting Information. Characterization of novel compounds, NMR spectra and chromatographic data are supplied as Supporting Information. This material is available free of charge via the Internet at http://pubs.acs.org.

AUTHOR INFORMATION

Corresponding Author

* E-mail: pher.andersson@su.se

Present Addresses

†If an author's address is different than the one given in the affiliation line, this information may be included here.

Author Contributions

The manuscript was written through contributions of all authors. / All authors have given approval to the final version of the manuscript. / ‡These authors contributed equally.

Funding Sources

Any funds used to support the research of the manuscript should be placed here (per journal style).

Notes

Any additional relevant notes should be placed here.

ACKNOWLEDGMENT

Energimyndigheten (The Swedish Energy Agency), Nordic Energy Research (N-INNER II), The Swedish Research Council (VR), The Knut and Alice Wallenberg Foundation, Stiftelsen Olle Engkvist Byggmästare and VR/SIDA for supporting this work. Mr. Jianguo Liu thanks the Guangzhou Elite Scholarship Council for a Ph.D. fellowship.

ABBREVIATIONS

CCR2, CC chemokine receptor 2; CCL2, CC chemokine ligand 2; CCR5, CC chemokine receptor 5; TLC, thin layer chromatography.

REFERENCES

[1] S. Goudedranche, W. Raimondi, X. Bugaut, T. Constantieux, D. Bonne, J. Rodriguez, *Synthesis* **2013**, *45*, 1909-1930.

[2] a) K. R. Fales, J. E. Green, P. K. Jadhav, D. P. Matthews, D. A. Neel, E. C. R. Smith, WO2007002181A2, **2007**; b) T. Kunchithapatham, S. Munusamy, B. R. Reguri, T. Sambashivam, S. Upparapalli, WO2012147020A1, **2012**.

[3] a) E. J. Corey, *Angew. Chem., Int. Ed.* **2002**, *41*, 1650-1667; b) S. Reymond, J. Cossy, *Chem. Rev.* **2008**, *108*, 5359-5406; c) H. L. Holmes, in *Organic Reactions*, John Wiley & Sons, Inc., **2004**; d) P. Merino, E. Marques-Lopez, T. Tejero, R. P. Herrera, *Synthesis* **2010**, 1-26.

[4] a) Y. Wang, H. Lu, P.-F. Xu, *Acc. Chem. Res.* **2015**, *48*, 1832-1844; b) S. Santra, P. R. Andreana, *Angew. Chem., Int. Ed.* **2011**, *50*, 9418-9422; c) L. F. Tietze, *Chem. Rev.* **1996**, *96*, 115-136.

[5] a) K. Takao, R. Munakata, K. Tadano, *Chem. Rev.* **2005**, *105*, 4779-4807; b) B. B. Toure, D. G. Hall, *Chem. Rev.* **2009**, *109*, 4439-4486.

[6] a) J. J. Verendel, O. Pamies, M. Dieguez, P. G. Andersson, *Chem. Rev.* **2014**, *114*, 2130-2169; b) A. Cadu, P. G. Andersson, *Dalton Transactions* **2013**, *42*, 14345-14356; c) Y. Chi, W. Tang, X. Zhang, in *Modern Rhodium-Catalyzed Organic Reactions*, Wiley-VCH Verlag GmbH & Co. KGaA, **2005**, pp. 1-31.

[7] a) J. J. Verendel, J. Q. Li, X. Quan, B. Peters, T. G. Zhou, O. R. Gautun, T. Govender, P. G. Andersson, *Chem-Eur J* **2012**, *18*, 6507-6513; b) L. Pauli, R. Tannert, R. Scheil, A. Pfaltz, *Chem.-Eur. J.* **2015**, *21*, 1482-1487; c) B. K. Peters, T. Zhou, J. Rujirawanich, A. Cadu, T. Singh, W. Rabten, S. Kerdphon, P. G. Andersson, *J. Am. Chem. Soc.* **2014**, *136*, 16557-16562; d) J.

Wysocki, N. Ortega, F. Glorius, *Angew. Chem., Int. Ed.* **2014**, *53*, 8751-8755; e) J. Wysocki, C. Schlepphorst, F. Glorius, *Synlett* **2015**, *26*, 1557-1562; f) W. Li, C. Schlepphorst, C. Daniliuc, F. Glorius, *Angew. Chem., Int. Ed.* **2016**, *55*, 3300-3303.

[8] a) R. D. Broene, S. L. Buchwald, *J. Am. Chem. Soc.* **1993**, *115*, 12569-12570; b) J. Blankenstein, A. Pfaltz, *Angew. Chem., Int. Ed.* **2001**, *40*, 4445-4447; c) Pier G. Cozzi, N. Zimmermann, R. Hilgraf, S. Schaffner, A. Pfaltz, *Adv. Synth. Catal.* **2001**, *343*, 450-454; d) S. Bell, B. Wüstenberg, S. Kaiser, F. Menges, T. Netscher, A. Pfaltz, *Science* **2006**, *311*, 642-644; e) S. Kaiser, S. P. Smidt, A. Pfaltz, *Angew. Chem., Int. Ed.* **2006**, *45*, 5194-5197; f) A. Trifonova, J. S. Diesen, P. G. Andersson, *Chem. - Eur. J.* **2006**, *12*, 2318-2328; g) M. Diéguez, J. Mazuela, O. Pàmies, J. J. Verendel, P. G. Andersson, *J. Am. Chem. Soc.* **2008**, *130*, 7208-7209; h) M. G. Schrems, A. Pfaltz, *Chem. Commun.* **2009**, 6210-6212; i) P. Tolstoy, M. Engman, A. Paptchikhine, J. Bergquist, T. L. Church, A. W. M. Leung, P. G. Andersson, *J. Am. Chem. Soc.* **2009**, *131*, 8855-8860; j) D. H. Woodmansee, M.-A. Muller, M. Neuburger, A. Pfaltz, *Chem. Sci.* **2010**, *1*, 72-78.

[9] P. Kaukoranta, M. Engman, C. Hedberg, J. Bergquist, P. G. Andersson, *Adv. Synth. Catal.* **2008**, *350*, 1168-1176.

[10] a) X. Cui, K. Burgess, *J. Am. Chem. Soc.* **2003**, *125*, 14212-14213; b) X. Cui, Y. Fan, M. B. Hall, K. Burgess, *Chem. - Eur. J.* **2005**, *11*, 6859-6868; c) J. Zhou, J. W. Ogle, Y. Fan, V. Banphavichit, Y. Zhu, K. Burgess, *Chem. - Eur. J.* **2007**, *13*, 7162-7170; d) J. Zhou, K. Burgess, *Angew. Chem., Int. Ed.* **2007**, *46*, 1129-1131.

[11] H. J. Jessen, A. Schumacher, T. Shaw, A. Pfaltz, K. Gademann, *Angew. Chem., Int. Ed.* **2011**, *50*, 4222-4226.

[12] Q.-L. Zhou, *Privileged Chiral Ligands and Catalysts*, Wiley-VCH Verlag GmbH & Co. KGaA, **2011**.

[13] A. Paptchikhine, K. Itto, P. G. Andersson, *Chem. Commun.* **2011**, *47*, 3989-3991.

[14] a) R. H. Crabtree, H. Felkin, G. E. Morris, *J. Chem. Soc., Chem. Commun.* **1976**, 716-717; b) R. H. Crabtree, *J. Chem. Soc., Chem. Commun.* **1975**, 647-648.

[15] Y. Zhu, Y. Fan, K. Burgess, *J. Am. Chem. Soc.* **2010**, *132*, 6249-6253.

[16] a) C. Wolf, D. H. Hochmuth, W. Koenig, C. Roussel, *Liebigs Ann.* **1996**, 357-363; b) C. Wolf, *Dynamic Stereochemistry of Chiral Compounds: Principles and Applications*, Royal Society of Chemistry, **2008**.

[17] Y. Zhu, K. Burgess, *Acc. Chem. Res.* **2012**, *45*, 1623-1636.

[18] R. Crabtree, *Acc. Chem. Res.* **1979**, *12*, 331-337.

[19] a) P. Brandt, C. Hedberg, P. G. Andersson, *Chem.-Eur. J.* **2003**, *9*, 339-347; b) X. Cui, Y. Fan, M. B. Hall, K. Burgess, *Chem.-Eur. J.* **2005**, *11*, 6859-6868; c) K. Källström, I. Munslow, P. G. Andersson, *Chem.-Eur. J.* **2006**, *12*, 3194-3200; d) Y. Fan, X. Cui, K. Burgess, M. B. Hall, *J. Am. Chem. Soc.* **2004**, *126*, 16688-16689.

[20] a) J. Mazuela, P.-O. Norrby, P. G. Andersson, O. Pàmies, M. Diéguez, *J. Am. Chem. Soc.* **2011**, *133*, 13634-13645; b) K. H. Hopmann, A. Bayer, *Organometallics* **2011**, *30*, 2483-2497; c) M. Sparta, C. Riplinger, F. Neese, *J. Chem. Theory Comput.* **2014**, *10*, 1099-1108; d) K. H. Hopmann, L. Frediani, A. Bayer, *Organometallics* **2014**, *33*, 2790-2797; e) K. H. Hopmann, *Int. J. Quantum Chem* **2015**, *115*, 1232-1249.

[21] S. Gruber, A. Pfaltz, *Angew. Chem., Int. Ed.* **2014**, *53*, 1896-1900.

[22] a) K. Källström, C. Hedberg, P. Brandt, A. Bayer, P. G. Andersson, *J. Am. Chem. Soc.* **2004**, *126*, 14308-14309; b) T. L. Church, T. Rasmussen, P. G. Andersson, *Organometallics* **2010**, *29*, 6769-6781.

[23] a) M. Mousseron, *Compt. rend.* **1942**, *215*, 201-203; b) H. L. Goering, W. W. Schmidt, V. D. Singleton, *J. Org. Chem.* **1979**, *44*, 2282-2284; c) G. Y. Ishmuratov, A. K. Shayakhmetova, M. P. Yakovleva, Y. V. Legostaeva, O. V. Shitikova, E. G. Galkin, G. A. Tolstikov, *Rus. J. Org. Chem.* **2007**, *43*, 1114-1119.

Insert Table of Contents artwork here

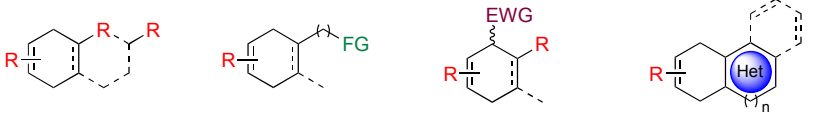

Minimally functionalised

Functionality on an extended chain

Ring tethered functionality

Heterocycle containing or heterocycle functionalised

R = Me, *n*-Bu, Ph, *i*-Pr, OMe
FG = OH, $OSiR_3$, $NHCOCF_3$
EWG = COOH, COOMe, $CONR_2$
Het = Pyrrole, Indole

44 examples, up to 99 % ee
Regioselective and high yielding

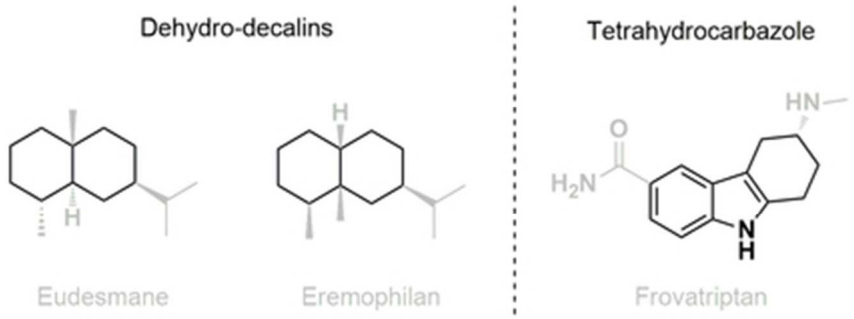

Figure 1

35x13mm (300 x 300 DPI)

Figure 2

17x4mm (300 x 300 DPI)

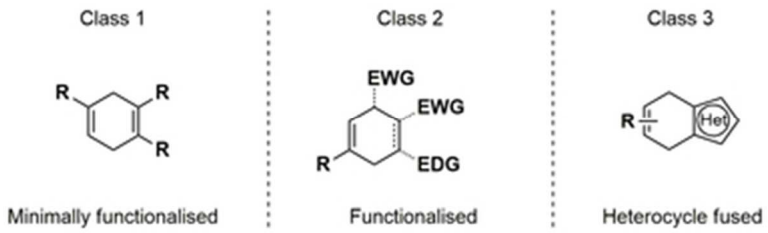

Figure 3

32x9mm (300 x 300 DPI)

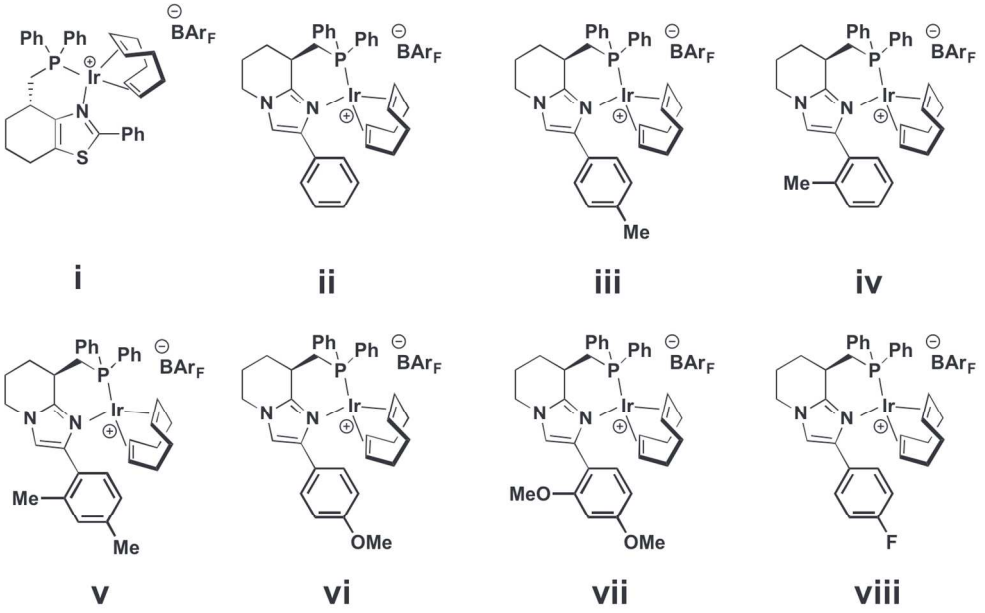

Figure 4

134x82mm (300 x 300 DPI)

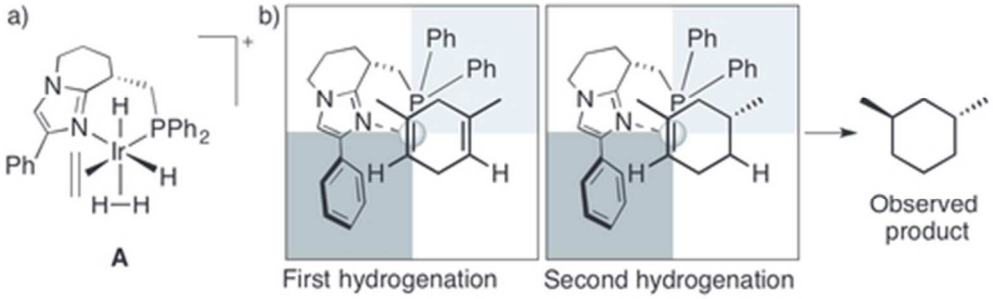

Figure 5

41x12mm (300 x 300 DPI)

Entry	Substrate	Product	i		ii		iii		iv		v		vi		vii		viii	
			conv.	ee (%)	conv.	ee (%)	conv.	ee (%)	conv.	ee (%)	conv.	ee (%)	conv.	ee (%)	conv.	ee (%)	conv.	ee (%)
1	 1a	 1b	99	92	99	79	99	81	99	67	**99**	**93**	99	65	**59**[d]	**94**	99	35
2	 2a	 2b	99	87	99	65	99	62	99	81	**99**	**86**	99	43	**99**	**94**	99	17
3	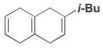 3a	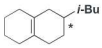 3b	99	92	99	65	99	78	99	88	**99**	**84**	99	59	**99**	**92**	99	26

Table 1

222x61mm (300 x 300 DPI)

Entry	Substrate	Product[b]	Catalyst	Yield (%)[c]	ee (%)[d]
1	 4a	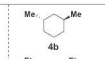 4b	v	99[e]	99
2	 5a	 5b	v	99[e,f]	94
3	 6a	 6b	v	99[e,f]	96
4	 7a	 7b	v	76[f]	99
5	 8a	 8b	v	91	99
6	 9a	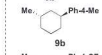 9b	v	81	99
7	 10a	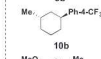 10b	v	99[e]	99
8	 11a	 11b	v	99[e]	99
9	 12a	 12b	v	99[e,f]	99
10	 13a	 13b	v	71[f]	98
11	 14a	 14b	v	68	99
12	 15a	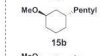 15b	i	81	98
13	 16a	 16b	v	95	99
14	 17a	 17b	v	99[e]	99
15	 18a	 18b	v	99[e]	94
16	 19a	 19b	v	99[e]	99
17	 20a	 20b	i	99[e]	98
18	 21a	 21b	v	99[e]	92
19	 22a	 22b	v	99[e]	98
20	 23a	 23b	v	82	98
21	24a	24b	i	98	99
22	25a	25b	v	72	99
23	1a	1b	v	97	93
24	2a	2b	vii	98	94
25	3a	3b	vii	98	92

Table 2

134x396mm (300 x 300 DPI)

Entry	Substrate	Product[b]	Catalyst	Yield (%)[c]	ee (%)[d]
1	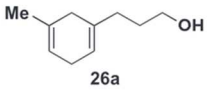 26a	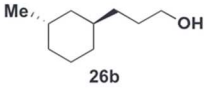 26b	v	84	99
2	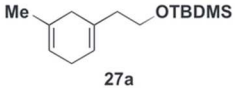 27a	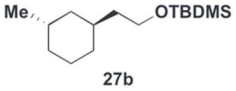 27b	v	86[e]	99
3	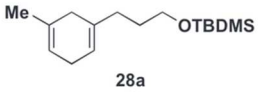 28a	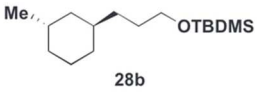 28b	v	87[e]	99
4	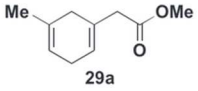 29a	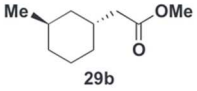 29b	ix[f]	97[e]	92
5	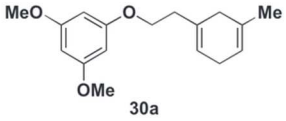 30a	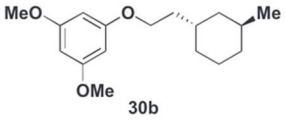 30b	v	79[e]	97

Table 3

92x57mm (300 x 300 DPI)

Entry	Substrate	Product[b]	Catalyst	Yield (%)[c]	ee (%)[d]
1	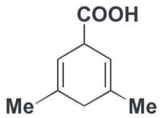 31a	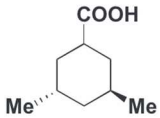 31b	**i**	91[e]	99
2	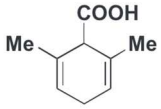 32a	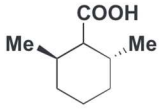 32b	**x**[f]	98[e]	99
3	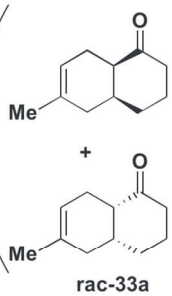 rac-33a	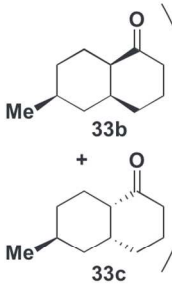 33b + 33c	**v**	98[g]	99
4	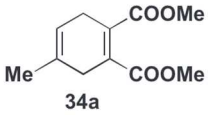 34a	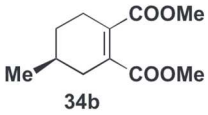 34b	**v**	99[h]	97

Table 4

124x105mm (300 x 300 DPI)

Entry	Substrate	Product[b]	Catalyst	Yield (%)[c]	ee (%)[d]
1	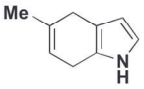 35a	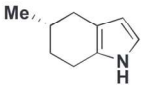 35b	v	98	99
2	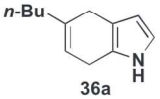 36a	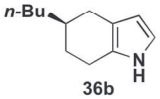 36b	i	85	90
3	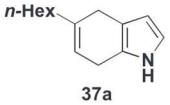 37a	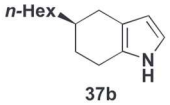 37b	i	83	92
4	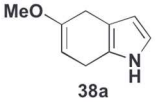 38a	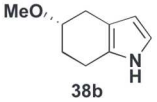 38b	v	99[e]	99
5	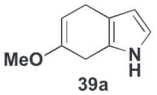 39a	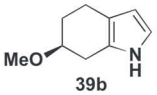 39b	v	99[e]	99
6	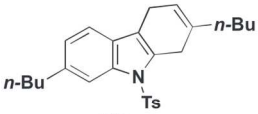 40a	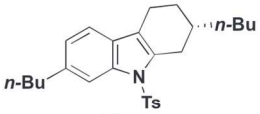 40b	ii	98	90
7	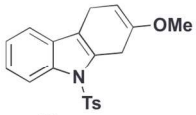 41a	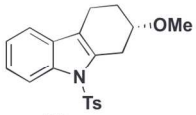 41b	v	99[e]	99
8	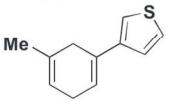 42a	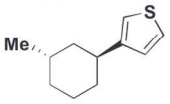 42b	i	99[e]	99

Table 5

140x146mm (300 x 300 DPI)

		pH_2/ bar	time/ min	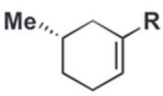 10c 42c	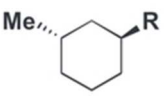 10b 42b
1	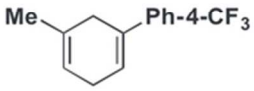 10a	5	30	94 (99% ee)	6
2	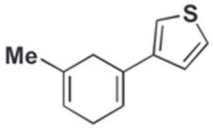 42a	50	300	83 (99% ee)	17

Table 6

59x30mm (300 x 300 DPI)

		Absolute configuration	
		predicted from mechanistic model	observed
1	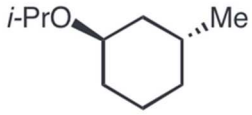 **13b**	(R)	(R)-(-)[22a]
2	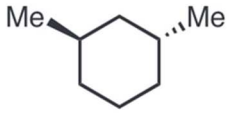 **4b**	(R)	(R)-(+)[22b]
3	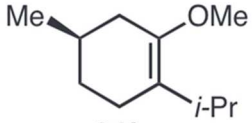 **21b**	(R)	(R)-(+)[b,22c]

Table 7

78x55mm (300 x 300 DPI)